RESEARCH ARTICLE

^{18}F-Florzolotau Tau Positron Emission Tomography Imaging in Patients with Multiple System Atrophy–Parkinsonian Subtype

Feng-Tao Liu, MD, PhD,[1] Xin-Yi Li, MD,[1] Jia-Ying Lu, MD,[2] Ping Wu, MD,[2] Ling Li, MD,[2] Xiao-Niu Liang, PhD,[1,3] Zi-Zhao Ju, MD,[2] Fang-Yang Jiao, MD,[2] Ming-Jia Chen, MD,[1] Jing-Jie Ge, MD, PhD,[2] Yi-Min Sun, MD, PhD,[1] Jian-Jun Wu, MD, PhD,[1] Tzu-Chen Yen, MD, PhD,[4] Jian-Feng Luo, PhD,[5] Chuantao Zuo, MD, PhD,[2*] Jian Wang, MD, PhD,[1*] and the Progressive Supranuclear Palsy Neuroimage Initiative (PSPNI)

[1]*Department of Neurology, National Research Center for Aging and Medicine, National Center for Neurological Disorders, and State Key Laboratory of Medical Neurobiology, Huashan Hospital, Fudan University, Shanghai, China*
[2]*PET Center, National Center for Neurological Disorders, and National Clinical Research Center for Aging and Medicine, Huashan Hospital, Huashan Hospital, Fudan University, Shanghai, China*
[3]*Institute of Neurology, Fudan University, Shanghai, China*
[4]*APRINOIA Therapeutics Co., Ltd, Suzhou, China*
[5]*Department of Biostatistics, School of Public Health, Fudan University, Shanghai, China*

ABSTRACT: Background: Anecdotal evidence suggests that patients diagnosed with the parkinsonian subtype of multiple system atrophy (MSA-P) may show uptake of the second-generation tau positron emission tomography (PET) tracer ^{18}F-Florzolotau (previously known as ^{18}F-APN-1607) in the putamen.
Objectives: This study systematically investigated the localization and magnitude of ^{18}F-Florzolotau uptake in a relatively large cohort of patients with MSA-P.
Methods: ^{18}F-Florzolotau PET imaging was performed in 31 patients with MSA-P, 24 patients with Parkinson's disease (PD), and 20 age-matched healthy controls. ^{18}F-Florzolotau signal in the striatum was analyzed by visual inspection and classified as either positive or negative. Regional ^{18}F-Florzolotau binding was also expressed as standardized uptake value ratio (SUVR) to assess whether it was associated with core symptoms of MSA-P after adjustment for potential confounders.
Results: By visual inspection and semiquantitative SUVR comparisons, patients with MSA-P showed elevated ^{18}F-Florzolotau uptake in the putamen, globus pallidus, and dentate—a finding that was not observed in PD. This increased signal was significantly associated with the core symptoms of MSA-P. In addition, patients with MSA-P with cerebellar ataxia showed an elevated ^{18}F-Florzolotau uptake in the cerebellar dentate.
Conclusions: ^{18}F-Florzolotau tau PET imaging findings may reflect the clinical severity of MSA-P and can potentially discriminate between this condition and PD. © 2022 International Parkinson and Movement Disorder Society.

Key Words: ^{18}F-Florzolotau; tau; positron emission tomography; multiple system atrophy; α-synucleinopathy

The term *neurodegenerative parkinsonism* is used to describe a group of neurodegenerative disorders that share similar clinical features despite different patterns of neuropathology.[1] The two main disease groups within the

*__Correspondence to:__ Prof. Jian Wang, Department of Neurology, Huashan Hospital, Fudan University, 12 Middle Wulumuqi Road, Shanghai 200040, China, E-mail: wangjian_hs@fudan.edu.cn; Prof. Chuantao Zuo, PET Center, Huashan Hospital, Fudan University, 518 East Wuzhong Road, Shanghai 200235, China, E-mail: zuochuantao@fudan.edu.cn

Feng-Tao Liu, Xin-Yi Li, and Jia-Ying Lu contributed equally to this work.

Relevant conflicts of interests/financial disclosures: Tzu-Chen Yen is an employee of APRINOIA Therapeutics Co., Ltd (Suzhou, China). All other authors have no conflicts of interest to declare.

Funding agencies: J.W. has received grants from the Shanghai Municipal Science and Technology Major Project (2018SHZDZX01 and 21S31902200) and the ZHANGJIANG LAB, a grant from National Health Commission of People Republic of China (Pro20211231084249000238), and grants from the National Natural Science Foundation of China (82171421 and 91949118). F.-T.L. has received funds (82171252 and 81701250) from the National Natural Science Foundation of China. C.Z. has received grants (82021002, 81971641, and 81671239) from the National Natural Science Foundation of China, the Research Project of Shanghai Health Commission (2020YJZX0111), and the Clinical Research Plan of Shanghai Hospital Development Center (No. SHDC2020CR1038B).

Received: 17 March 2022; **Revised:** 24 June 2022; **Accepted:** 29 June 2022

Published online in Wiley Online Library (wileyonlinelibrary.com). DOI: 10.1002/mds.29159

spectrum of parkinsonism are α-synucleinopathies—including Parkinson's disease (PD), multiple system atrophy (MSA), and Lewy body dementia[2-4]—and tauopathies—comprising progressive supranuclear palsy (PSP), corticobasal syndrome,[1,5] and frontotemporal dementia associated with mutations in the microtubule-associated protein tau gene (*MAPT*).[6] Unfortunately, the considerable overlap of signs and symptoms between these conditions—especially in the early stage—poses significant diagnostic challenges. In this scenario, imaging-based biomarkers for diagnosis and clinical decision making in the field of neurodegenerative parkinsonism are highly sought after.

In addition to traditional positron emission tomography (PET) tracers of dopaminergic dysfunction and glucose metabolism, new experimental probes have been recently tested in neurodegenerative parkinsonism.[7-9] We have previously described a putamen uptake of the second-generation tau tracer ^{18}F-Florzolotau (previously known as ^{18}F-APN-1607 or ^{18}F-PM-PBB3) in four of seven patients diagnosed with the parkinsonian subtype of MSA (MSA-P)[10]—a rare condition classified as an α-synucleinopathy. Conversely, this binding was not observed among patients with PD.[10] Similar findings were subsequently reported by Cho and colleagues,[11] who found a significant uptake of the first-generation tau tracer ^{18}F-AV-1451 in the posterior putamen of four patients with a diagnosis of probable MSA-P. This was not attributed to tracer binding to α-synuclein but to its off-target accumulation in iron deposits.[11] In another study, Perez-Soriano and colleagues[12] described an uptake of ^{11}C-PBB3 in the frontal lobe, globus pallidus, midbrain, parietal lobe, putamen, temporal lobe, substantia nigra, thalamus, and ventral striatum of a patient with MSA. Koga and colleagues[13] have interpreted the ^{11}C-PBB3 binding in a subset of patients with MSA as a result of the ability of the tracer to accumulate within areas where glial cytoplasmic inclusions—the defining neuropathological feature of MSA—are highly dense. On analyzing ^{18}F-THK-5351 tau PET images obtained in nine patients with MSA-P, Schonecker and colleagues[14] found an increased tracer uptake in the lentiform nucleus—albeit without significant differences compared with other parkinsonian disorders.

Starting from these pilot observations, we undertook this study to shed further light on the localization and magnitude of ^{18}F-Florzolotau uptake in a relatively large cohort of patients with MSA-P. We also investigated the associations between ^{18}F-Florzolotau PET imaging parameters and the core clinical symptoms of this neurodegenerative parkinsonism.

Patients and Methods

Study Participants

Patients with MSA-P (n = 31) and PD (n = 24) were recruited from the Movement Disorders Clinic, Department of Neurology, Huashan Hospital, Fudan University (Shanghai, China) between October 2020 and August 2021. All clinical diagnoses were made by neurologists specializing in the field of movement disorders (Y.-M.S., J.-J.W., and J.W.) based on established diagnostic criteria for MSA[15] and PD.[16] For the purpose of comparison, 20 age-matched healthy controls (HCs) were also included. Subjects who had a positive history of neurological or psychiatric disorders, who showed neurological deficits on physical examination, or had abnormal findings on brain magnetic resonance imaging were not eligible as HCs. Ethical approval was obtained from the Institutional Review Board of the Huashan Hospital (reference number: KY2019-433). All participants provided written informed consent before enrollment.

Clinical Evaluation

All patients with MSA-P and PD underwent clinical assessments at least 12 hours after withdrawal of their normal antiparkinsonian drug therapy. The clinical evaluation consisted of measures of global cognition (Mini-Mental State Examination) and motor symptoms (Movement Disorder Society–Sponsored Revision of the Unified Parkinson's Disease Rating Scale [MDS UPDRS] and Hoehn and Yahr scale [H&Y]). The disease-specific assessment of MSA-P severity was performed using the Unified Multiple System Atrophy Rating Scale (UMSARS), including a historical review of disease-related impairments (Part I, 12 items), motor examination (Part II, 14 items), autonomic examination (Part III), and global disability scale (Part IV).[17] Higher scores indicate worse clinical manifestations. The total levodopa equivalent daily dose (LEDD) was also calculated. All of the clinical data were reviewed by an expert panel. Upon completion of the clinical visits, participants underwent ^{18}F-Florzolotau tau PET imaging.

Image Acquisition

All images were acquired in Huashan Hospital by experienced radiologists who were blinded to the clinical data. Patients initially underwent anatomical magnetic resonance imaging (MRI) in a 3.0-T horizontal magnet (Discovery MR750; GE Medical Systems, Milwaukee, WI) followed by static ^{18}F-Florzolotau tau PET imaging using a 20-minute acquisition protocol (90–110 minutes) (mCT Flow PET/computed tomography; Siemens Healthcare GmbH, Erlangen, Germany). The procedure for image acquisition has been previously described in detail.[10,18] The tosylate precursor used for the radiosynthesis of ^{18}F-Florzolotau was obtained from APRINOIA Therapeutics (Suzhou, China).[10]

Image Processing

The original images were converted into the Nifti format using the MRIcroN script. Following coregistration of PET and T1-weighted MRI data, PET images were normalized to the Montreal Neurological Institute space to obtain the spatial transformation matrix. Normalized PET images were subsequently smoothed with a Gaussian kernel with a full width at half maximum of 6 mm. Using the cerebellar gray matter as the reference region, standardized uptake value ratio (SUVR) maps were obtained for semiquantification of tracer deposition. SUVR values were calculated by setting the following 16 regions of interest: frontal cortex, parietal cortex, occipital cortex, temporal cortex, caudate, putamen, globus pallidus, thalamus, subthalamic nucleus, tegmentum, substantia nigra, red nucleus, pontine base, raphe nuclei, locus coeruleus, and dentate nucleus.[10] Mean values obtained from bilateral measurements were used for the purpose of analysis.[10] All procedures were carried out using the Statistical Parametric Mapping toolbox (version 12; http://www.fil.ion.ucl.ac.uk/spm/software/spm12/) implemented in MATLAB (MathWorks, Natick, MA).

Visual Image Interpretation

Visual interpretation of ^{18}F-Florzolotau PET images was performed by three independent assessors, including two experienced neuroradiologists with specific expertise in neurodegenerative disorders (C.Z., more than 20 years of experience; J.-Y.L., more than 5 years of experience) and a neurologist specializing in neuroimaging (F.-T.L., more than 10 years of experience). All assessors were blinded to the clinical diagnoses. ^{18}F-Florzolotau images were displayed with the Mango viewer software (version 4.1; Research Imaging Institute, The University of Texas Health Science Center, San Antonio, TX; http://ric.uthscsa.edu/mango). We manually adjusted the maximum intensity so that the predominant color in the inferior cerebellar cortex would be the midpoint of the spectrum color scale. Images were evaluated in the transverse, sagittal, and coronal views and visually assessed in the striatum. Using the syngo application (Siemens Healthcare GmbH), ^{18}F-Florzolotau tau PET images were also displayed in the three-dimensional mode and inverted to a range of grayscale values. The maximum intensity of the scale was manually adjusted to 40% of the individual maximum raw intensity. The tracer uptake in the striatum was classified as either positive or negative based on the consensus of at least two independent assessors.

Calculation of SUVR *z* Scores

Regional SUVR z scores were calculated according to the following formula: z score = (individual patient's SUVR − mean SUVR value observed in HCs)/standard deviation (SD) of the SUVR value observed in HCs. For semiquantitative interpretation of the findings, a regional z score ≥2 was considered to define positivity.[10,19]

Data Analysis

Prior to the analysis, continuous data were checked for normal distribution using the Kolmogorov–Smirnov test. Skewed variables are expressed as medians and interquartile ranges, whereas normally distributed data are summarized as means ± standard deviations. The F test was used to determine the homogeneity of variance. Student's t tests and Mann–Whitney U tests were used to test for differences in normally distributed and skewed continuous variables between two groups, respectively. Three-group comparisons were untaken using one-way analysis of variance and Kruskal–Wallis tests, as appropriate, with post hoc Bonferroni's correction and pairwise comparisons for normally distributed and skewed data, respectively. To analyze categorical variables, χ^2 tests were used. A generalized linear model (GLM) was applied to examine the intergroup differences in terms of semiquantitative PET results across different target regions after adjustment for age, sex, disease duration, and MDS UPDRS Part III scores. The thresholds of significance in the GLM were adjusted for multiple comparisons using the Benjamini–Hochberg procedure. To investigate the associations between clinical variables and SUVR values of target areas, Pearson's correlation coefficients were calculated. Partial correlation analysis was performed to identify the statistically significant correlations between PET findings and the clinical features of patients with MSA-P after adjustment for age, education, and LEDD. No correction for multiple comparisons was applied. All calculations were undertaken with SPSS for Windows (version 22.0; IBM Corp., Armonk, NY). Two-tailed P values <0.05 were considered statistically significant.

Results

General Characteristics of the Three Study Groups

The general characteristics of the three study groups are summarized in Table 1. Compared with patients with MSA-P and PD, HCs had a greater prevalence of women and showed both higher education and better cognition. However, the three groups were well matched in terms of age. Compared with patients with PD, those patients with MSA-P had a longer disease duration (albeit not significantly so), a higher motor severity (MDS UPDRS Part III and H&Y scores), and higher LEDD (although without reaching the threshold for statistical significance).

TABLE 1 *General characteristics of the three study groups*

	Patients with MSA-P	Patients with PD	Healthy controls	*P*	Post hoc *P*
Number of subjects	31	24	20	–	–
Sex, men/women	14/17	16/8	6/14	0.049	0.330,[a] 0.850,[b] 0.047[c]
Age, years	60.32 ± 6.02	60.75 ± 14.14	56.60 ± 7.11	0.299	1.000,[a] 0.543,[b] 0.474[c]
Education, years	8.65 ± 4.10	8.50 ± 3.73	12.25 ± 3.24	0.002	1.000,[a] 0.004,[b] 0.005[c]
MMSE	26.00 (21.00–28.00)	25.00 (22.00–28.00)	28.00 (27.00–29.00)	0.006	1.000,[a] 0.021,[b] 0.009[c]
Duration of disease, months	32.00 (20.00–41.00)	21.00 (12.25–53.25)	–	0.231	–
MDS UPDRS Part III	51.77 ± 11.94	43.13 ± 15.80	–	0.026	–
H&Y	3.0 (3.0–4.0)	3.0 (2.0–3.0)	–	0.023	–
LEDD	600.00 (450.00–700.00)	337.50 (25.00–691.25)	–	0.079	–

Data are expressed as mean ± standard deviation or median (interquartile range). Post hoc *P* values were calculated after application of the Bonferroni's correction.
[a]Patients with MSA-P versus patients with PD.
[b]Patients with MSA-P versus healthy controls.
[c]Patients with PD versus healthy controls.
Abbreviations: MSA-P, multiple system atrophy–parkinsonian subtype; PD, Parkinson's disease; MMSE, Mini-Mental State Examination; MDS UPDRS, Movement Disorders Society Unified Parkinson's Disease Rating Scale; H&Y, Hoehn and Yahr scale; LEDD, levodopa equivalent daily dose.

Visual Interpretation of ^{18}F-Florzolotau Tau PET Images in Patients with MSA-P

On visual analysis of individual images, the presence of a striatum-dominant ^{18}F-Florzolotau pattern effectively distinguished patients with MSA-P (31/31; Fig. 1, left of the dashed line, and Video S1) from those with PD (2/24; Video S2) and HCs (0/20). In addition, the presence of an increased tracer accumulation in the putamen, globus

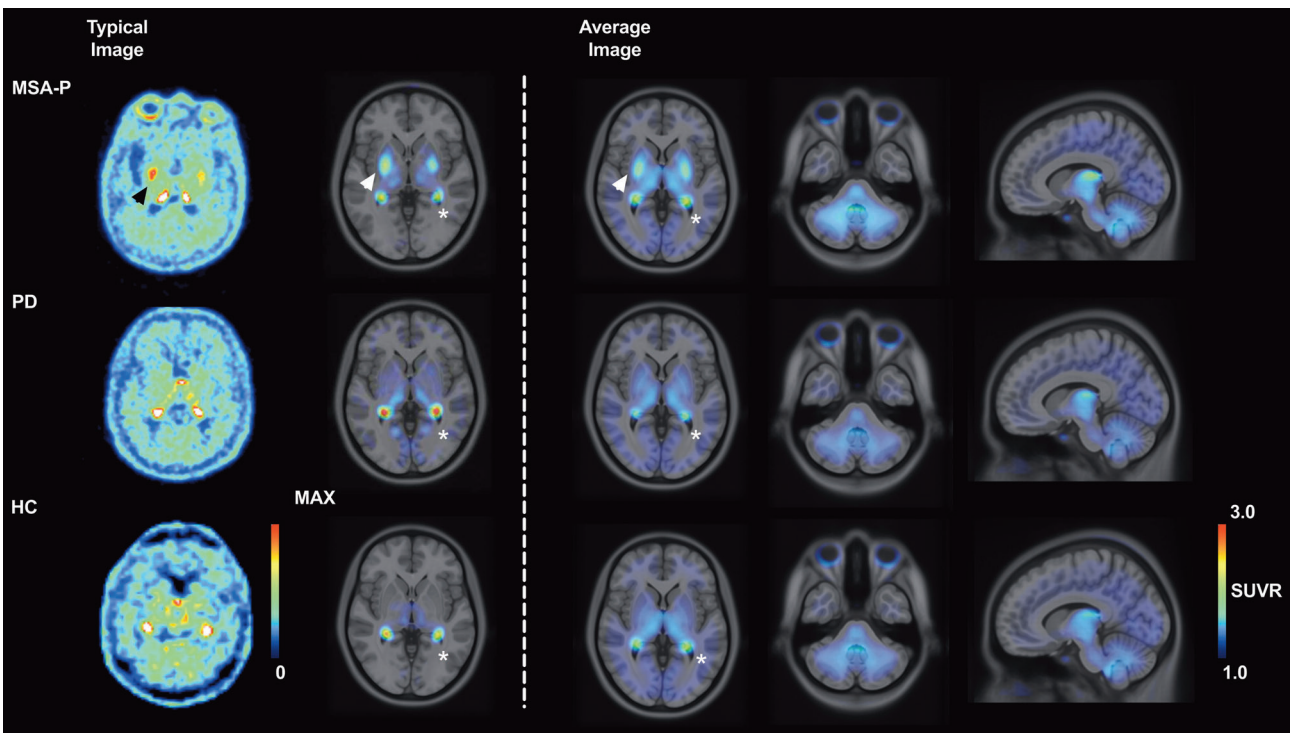

FIG. 1. ^{18}F-Florzolotau binding patterns in patients with MSA-P and PD and HCs. Individual and group data are reported on the left and right sides of the vertical dashed line, respectively. Illustrative findings from a 68-year-old male patient with MSA-P (case 6; disease duration: 24 months; left upper raw), a 58-year-old male patient with PD (case 53; disease duration: 68 months; left middle raw), and a 62-year-old female HC (left lower raw). On averaged SUVR images, patients with MSA-P showed an obvious tracer accumulation in the putamen and globus pallidus as well as a mildly increased uptake in the cerebellum. Arrow, putamen; *choroid plexus. HC, healthy control; MSA-P, multiple system atrophy–parkinsonian subtype; PD, Parkinson's disease; SUVR, standardized uptake value ratio. [Color figure can be viewed at wileyonlinelibrary.com]

pallidus, and—to a lesser extent—the cerebellum was confirmed at a group level (Fig. 1, right of the dashed line).

Regional SUVR Values in the Three Study Groups

The heatmap of regional SUVR values is shown in Figure S1. Compared with HCs, patients with MSA-P showed significantly higher ^{18}F-Florzolotau SUVR values in the putamen ($P < 0.001$), globus pallidus ($P < 0.001$), and cerebellar dentate ($P < 0.01$). All of the differences maintained their statistical significance after correction for multiple comparisons. The SUVR values of the cortex, thalamus, and brainstem did not differ significantly between patients with MSA-P and HCs. Compared with patients with PD, the SUVR values of the brainstem were slightly increased in those with MSA-P ($P < 0.01$; Table 2). SUVR z scores of the putamen, globus pallidus, and dentate were significantly higher in patients with MSA-P compared with those with PD and HCs (Fig. 2A). The heatmap of regional z scores in the three study groups is shown in Figure 2B. The criteria for positivity in the putamen, globus pallidus, and dentate nucleus were met by 61.3% (19/31) of patients with MSA-P; specifically, 38.7% (12/31), 38.7% (12/31), and 32.3% (10/31) of patients diagnosed with MSA-P had positive results in the putamen, globus pallidus, and dentate, respectively. Neither patients with PD nor HCs showed positive ^{18}F-Florzolotau tau PET findings in these regions (Fig. S2).

Associations Between ^{18}F-Florzolotau Binding Patterns and the Clinical Characteristics of Patients with MSA-P

In patients with MSA-P, the SUVR value in the putamen was positively associated with age ($r = 0.525$, $P = 0.002$); a similar correlation was observed for the SUVR value in the globus pallidus, albeit not significantly so ($r = 0.331$, $P = 0.069$). After adjustment for age, education, and LEDD in partial correlation analyses uncorrected for multiple comparisons, the SUVR value in the globus pallidus showed positive associations with the UMSARS Part I score ($r = 0.404$,

TABLE 2 *Standardized uptake value ratios of ^{18}F-Flozolotau uptake in different brain regions according to the clinical diagnosis*

Brain region	Patients with MSA-P	Patients with PD	Healthy controls	*P*	*P*⋆	*P*⋆⋆	*P*⋆⋆⋆
Frontal cortex	0.93 ± 0.07	0.93 ± 0.07	0.94 ± 0.07	0.813	0.907	0.702	0.356
Parietal cortex	0.95 ± 0.08	0.95 ± 0.09	0.94 ± 0.06	0.806	0.907	0.935	0.900
Occipital cortex	1.06 ± 0.06	1.07 ± 0.09	1.06 ± 0.07	0.758	0.987	0.857	0.935
Temporal cortex	1.02 ± 0.08	1.03 ± 0.11	1.01 ± 0.06	0.790	0.974	0.974	0.753
Caudate	0.90 ± 0.13	0.85 ± 0.15	0.94 ± 0.09	0.058	0.843	0.157	0.083
Putamen	1.39 ± 0.12	1.20 ± 0.11	1.17 ± 0.11	<0.001	<0.001[a]	0.669	<0.001[b]
Globus pallidus	1.50 ± 0.12	1.30 ± 0.12	1.27 ± 0.13	<0.001	<0.001[a]	0.825	<0.001[b]
Thalamus	1.53 ± 0.20	1.41 ± 0.22	1.44 ± 0.16	0.068	0.388	0.825	0.062
Subthalamic nucleus	1.44 ± 0.12	1.38 ± 0.16	1.37 ± 0.13	0.124	0.157	0.996	0.157
Tegmentum	1.42 ± 0.10	1.34 ± 0.10	1.37 ± 0.11	0.017	0.135	0.859	0.022[b]
Substantia nigra	1.35 ± 0.12	1.27 ± 0.11	1.31 ± 0.14	0.050	0.318	0.759	0.016
Red nucleus	1.44 ± 0.11	1.39 ± 0.13	1.39 ± 0.10	0.156	0.145	0.996	0.215
Pontine base	1.26 ± 0.12	1.19 ± 0.10	1.23 ± 0.14	0.069	0.603	0.603	0.020[b]
Raphe nuclei	1.38 ± 0.11	1.31 ± 0.10	1.33 ± 0.11	0.024	0.135	0.907	0.028
Locus coeruleus	1.32 ± 0.11	1.27 ± 0.11	1.28 ± 0.13	0.177	0.201	0.907	0.052
Dentate nucleus	1.50 ± 0.19	1.32 ± 0.11	1.35 ± 0.13	<0.001	0.028[a]	0.289	0.002[b]

Data are expressed as mean ± standard deviation. *P* values for pairwise comparisons of the three study groups were adjusted for multiple comparisons using the Benjamini–Hochberg procedure.

⋆Patients with MSA-P versus healthy controls.

⋆⋆Patients with PD versus healthy controls.

⋆⋆⋆Patients with MSA-P versus patients with PD.

[a]Statistically significant result after applying the post hoc correction for multiple comparisons and adjustment for age and sex.

[b]Statistically significant result after applying the post hoc correction for multiple comparisons and adjustment for age, sex, disease duration, and Movement Disorders Society Unified Parkinson's Disease Rating Scale Part III scores.

Abbreviations: MSA-P, multiple system atrophy–parkinsonian subtype; PD, Parkinson's disease.

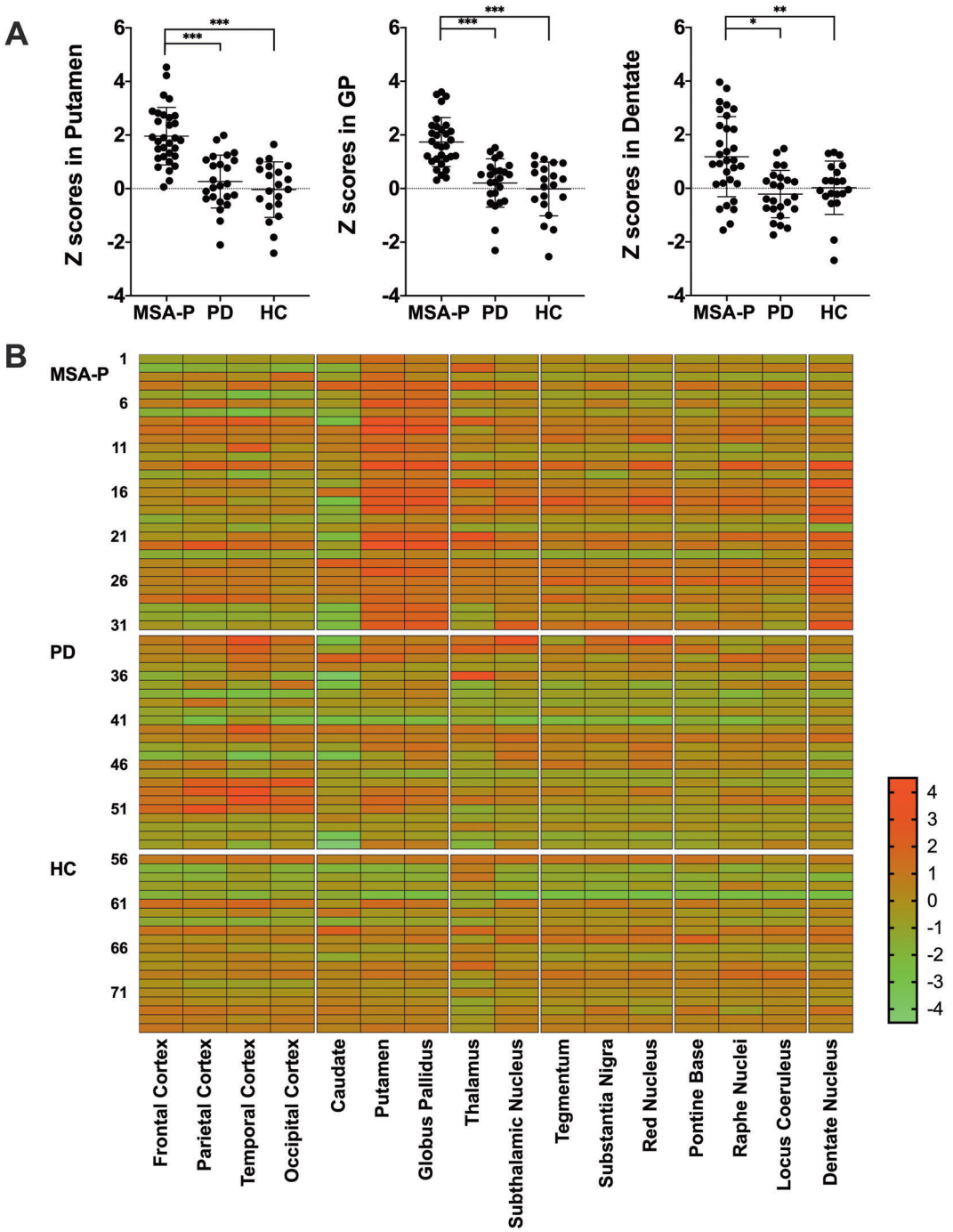

FIG. 2. Regional ^{18}F-Florzolotau uptake differences in the three study groups. (A) standardized uptake value ratio *z* scores in the putamen, globus pallidus, and dentate were significantly higher in patients with MSA-P compared with both patients with PD and HC. (B) Heatmap of standardized uptake value ratio *z* scores in the three study groups. **P* < 0.05; ***P* < 0.01; ****P* < 0.001. GP, globus pallidus; HC, healthy control; MSA-P, multiple system atrophy–parkinsonian subtype; PD, Parkinson's disease. [Color figure can be viewed at wileyonlinelibrary.com]

$P = 0.033$) and the UMSARS Part II score ($r = 0.439$, $P = 0.019$). When the same adjustments were applied, the SUVR value in the putamen was positively associated with the UMSARS Part I score ($r = 0.377$, $P = 0.048$) and the UMSARS Part II score ($r = 0.385$, $P = 0.043$; Fig. 3A).

SUVR Values in Patients with MSA-P According to the Presence or Absence of Cerebellar Ataxia

The general characteristics of patients of MSA-P according to the presence or absence of cerebellar ataxia are shown in Table S1. Notably, the SUVR

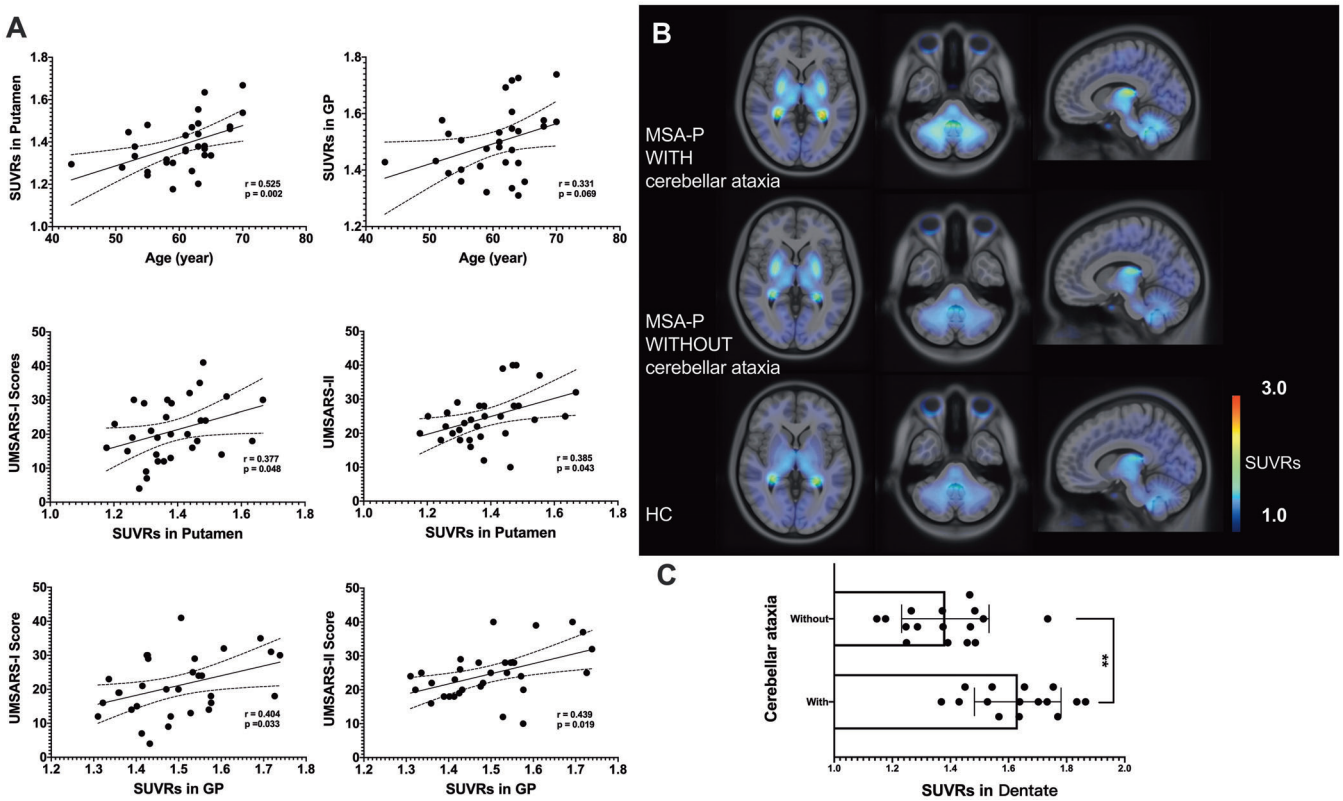

FIG. 3. Associations between ^{18}F-Florzolotau binding patterns and the clinical characteristics of patients with MSA-P. (A) Correlations between ^{18}F-Florzolotau binding patterns and age, UMSARS Part I, and UMSARS Part II. (B) Group-average images of patients with MSA-P according to the presence or absence of cerebellar ataxia. (C) SUVR values in the cerebellar dentate were significantly higher in patients with cerebellar ataxia compared with those without. $^{**}P < 0.01$. GP, globus pallidus; HC, healthy control; MSA-P, multiple system atrophy–parkinsonian subtype; SUVR, standardized uptake value ratio; UMSARS, Unified Multiple System Atrophy Rating Scale. [Color figure can be viewed at wileyonlinelibrary.com]

values in those with cerebellar ataxia were significantly higher compared with those without ($P < 0.01$), especially in the cerebellar dentate nucleus (Fig. 3B,C and Table S2).

Discussion

This is, to our knowledge, the first study to systematically investigate ^{18}F-Florzolotau tau PET imaging findings in a relatively large cohort of patients with MSA-P. We found that a diagnosis of MSA-P was associated with an increased ^{18}F-Florzolotau uptake in the putamen, globus pallidus, and dentate—a pattern that was not observed in PD, another α-synucleinopathy. We also demonstrated that the higher ^{18}F-Florzolotau accumulation in the putamen, globus pallidus, and dentate was significantly associated with the core symptoms of MSA-P. The spatial distribution of the ^{18}F-Florzolotau signal in the putamen and globus pallidus appeared unbiased on visual inspections; in addition, on analyzing the SUVR z scores, 14 (45.2%) patients with MSA-P met the criteria for positivity in the putamen and/or globus pallidus. Collectively, our results indicate that ^{18}F-Florzolotau tau PET imaging may be clinically useful even in a disorder that cannot be classified as a tauopathy.

Using a second-generation tau tracer, our study expands previous anecdotal evidence of positive PET tau signals in MSA[11,12,14] and suggests that ^{18}F-Florzolotau tau PET imaging may have diagnostic potential in MSA-P.[10] Future research will be needed to examine more rigorously the clinical utility of ^{18}F-Florzolotau PET imaging in the differential diagnosis of parkinsonism.

However, the potential reasons underlying the increased uptake of a PET tau tracer in a disease classified as an α-synucleinopathy merit comment. An autopsy study reported that four-repeat (4R)-tau-positive granules can be commonly seen in glial cells of MSA brains, especially in the putamen and globus pallidus.[20] Although ^{18}F-Florzolotau appears to have high affinity for 4R-tau proteins,[21] the possibility that the observed tracer retention in MSA-P brains could be attributed to tau-positive granules in the glia deserves further scrutiny. Neuroinflammation has been previously associated with the presence of tau pathology—being in turn linked to clinical severity[22] and the clinical trajectories of PSP.[23] Neuroinflammatory reactions have also been implicated in the pathogenesis of

MSA.[24,25] Future work combining the use of ^{18}F-Florzolotau and other tracers of neuroinflammation (eg, ^{11}C-PK11195) may shed more light on the link between ^{18}F-Florzolotau binding and the occurrence of neuroinflammatory reactions in MSA-P.

Another potential explanation may lie in the possible binding of ^{18}F-Florzolotau to α-synuclein. A previous in vitro investigation found that ^{11}C-PBB3, a first-generation tau tracer, might recognize the α-synuclein deposits typical of MSA-P.[13] However, no autopsy study has confirmed that ^{18}F-Florzolotau may bind to α-synuclein in MSA. To our knowledge, only one postmortem study conducted in patients with dementia with Lewy bodies investigated the binding affinity of ^{18}F-Florzolotau for α-synuclein. The results revealed that the affinity of this tracer was relatively low for α-synuclein but high for Alzheimer's disease–type protein fibrils.[26] Furthermore, the magnitude of ^{18}F-Florzolotau accumulation observed in PD—another α-synucleinopathy—was substantially limited. Although no direct evidence was provided of ^{18}F-Florzolotau binding to α-synuclein, caution should be exercised in light of the different α-synuclein isoforms involved in the development of MSA-P and PD.[27]

In our study, SUVR values in certain subcortical regions were >1.2—even in cognitively HCs. In a recent large study (n = 19,097) conducted by the Amyloid Biomarker Study Group, imaging and cerebrospinal fluid biomarkers of amyloid pathology increased in parallel with age, regardless of the presence of normal cognition versus subjective cognitive decline.[28] We therefore believe that the mild ^{18}F-Florzolotau uptake observed in control subjects and in certain subcortical regions can be attributed to age-related tau depositions.

Although our single-center study is limited by the inability to perform postmortem investigations that would elucidate the possible binding target for ^{18}F-Florzolotau in patients with MSA-P, our results may have significant clinical implications. First, we expanded previous findings on the usefulness of ^{18}F-Florzolotau tau PET imaging for distinguishing between MSA-P and PSP[10,18] by showing that this platform may also discriminate MSA-P from PD (Video S1). Second, the magnitude of the ^{18}F-Florzolotau signal in the putamen and globus pallidus was associated with disease severity, while binding in the cerebellar dentate was associated with the presence of cerebellar ataxia. However, these results must be interpreted cautiously as correlation analyses were unadjusted for multiple comparisons. If independently validated, these findings may pave the way for the use of ^{18}F-Florzolotau tau PET imaging findings as a biomarker for the variable clinical expressiveness of MSA-P. Interestingly, a recent study demonstrated that the presence of tau-positive granules in glial cells in patients with MSA is associated with long disease duration and the requirement of long-term tube feeding and/or tracheotomy.[29] Further research on the reciprocal interactions between ^{18}F-Florzolotau binding sites, postmortem neuropathological features, and disease severity is warranted. In addition, prospective longitudinal studies in which patients with MSA-P are reassessed periodically with ^{18}F-Florzolotau PET imaging are required to examine whether an increased tracer uptake occurs over time and if this would correlate with clinical progression.

In summary, we observed that, despite ^{18}F-Florzolotau being a tau tracer, patients with MSA-P—an α-synucleinopathy—demonstrated elevated signals localized in the striatum, thus offering the possibility that ^{18}F-Florzolotau tau PET imaging may be helpful for differential diagnosis with PD. In addition, the amount of ^{18}F-Florzolotau uptake was found to correlate with clinical features and severity of MSA-P—a result that requires confirmation in longitudinal investigations. ■

Acknowledgments: We express our gratitude to all of the study participants and their relatives. We are grateful to APRINOIA Therapeutics for the provision of the ^{18}F-Florzolotau precursor. We thank Xi-Xi Han, Yi Chen, Ying-Jun Hu, and Jia Zhang (PAWEI Health Promotion Center for Parkinsonism, Shanghai, China) for volunteering in the study.

Data Availability Statement

The datasets generated during and/or analyzed during the current study are available from the corresponding author on reasonable request.

References

1. Jabbari E, Holland N, Chelban V, et al. Diagnosis across the spectrum of progressive supranuclear palsy and corticobasal syndrome. JAMA Neurol 2020;77(3):377–387.
2. Goedert M. Alpha-synuclein and neurodegenerative diseases. Nat Rev Neurosci 2001;2(7):492–501.
3. Wenning GK, Colosimo C, Geser F, Poewe W. Multiple system atrophy. Lancet Neurol 2004;3(2):93–103.
4. Outeiro TF, Koss DJ, Erskine D, et al. Dementia with lewy bodies: an update and outlook. Mol Neurodegener 2019;14(1):5
5. Rosler TW, Tayaranian Marvian A, Brendel M, et al. Four-repeat tauopathies. Prog Neurobiol 2019;180:101644
6. Dickson DW, Kouri N, Murray ME, Josephs KA. Neuropathology of frontotemporal lobar degeneration-tau (FTLD-tau). J Mol Neurosci 2011;45(3):384–389.
7. Lyoo CH, Cho H, Choi JY, Ryu YH, Lee MS. Tau positron emission tomography imaging in degenerative Parkinsonisms. J Mov Disord 2018;11(1):1–12.
8. Strafella AP, Bohnen NI, Perlmutter JS, et al. Molecular imaging to track Parkinson's disease and atypical parkinsonisms: new imaging frontiers. Mov Disord 2017;32(2):181–192.
9. Saint-Aubert L, Lemoine L, Chiotis K, Leuzy A, Rodriguez-Vieitez E, Nordberg A. Tau PET imaging: present and future directions. Mol Neurodegener 2017;12(1):19
10. Li L, Liu F-T, Li M, et al. Clinical utility of 18F-APN-1607 tau PET imaging in patients with progressive supranuclear palsy. Mov Disord 2021;36(10):2314–2323.
11. Cho H, Choi JY, Lee SH, Ryu YH, Lee MS, Lyoo CH. ^{18}F-AV-1451 binds to putamen in multiple system atrophy. Mov Disord 2017;32(1):171–173.

12. Perez-Soriano A, Arena JE, Dinelle K, et al. PBB3 imaging in parkinsonian disorders: evidence for binding to tau and other proteins. Mov Disord 2017;32(7):1016–1024.
13. Koga S, Ono M, Sahara N, Higuchi M, Dickson DW. Fluorescence and autoradiographic evaluation of tau PET ligand PBB3 to alpha-synuclein pathology. Mov Disord 2017;32(6):884–892.
14. Schonecker S, Brendel M, Palleis C, et al. PET imaging of astrogliosis and tau facilitates diagnosis of parkinsonian syndromes. Front Aging Neurosci 2019;11:249
15. Gilman S, Wenning GK, Low PA, et al. Second consensus statement on the diagnosis of multiple system atrophy. Neurology 2008;71(9):670–676.
16. Postuma RB, Berg D, Stern M, et al. MDS clinical diagnostic criteria for Parkinson's disease. Mov Disord 2015;30(12):1591–1601.
17. Wenning GK, Tison F, Seppi K, et al. Development and validation of the unified multiple system atrophy rating scale (UMSARS). Mov Disord 2004;19(12):1391–1402.
18. Tagai K, Ono M, Kubota M, et al. High-contrast in vivo imaging of tau pathologies in Alzheimer's and non-Alzheimer's disease Tauopathies. Neuron 2021;109(1):42–58 e8.
19. Brendel M, Barthel H, van Eimeren T, et al. Assessment of 18F-PI-2620 as a biomarker in progressive supranuclear palsy. JAMA Neurol 2020;77(11):1408–1419.
20. Nagaishi M, Yokoo H, Nakazato Y. Tau-positive glial cytoplasmic granules in multiple system atrophy. Neuropathology 2011;31(3):299–305.
21. Su Y, Fu J, Yu J, et al. Tau PET imaging with [18F]PM-PBB3 in frontotemporal dementia with MAPT mutation. J Alzheimers Dis 2020;76(1):149–157.
22. Malpetti M, Passamonti L, Rittman T, et al. Neuroinflammation and tau colocalize in vivo in progressive supranuclear palsy. Ann Neurol 2020;88(6):1194–1204.
23. Malpetti M, Passamonti L, Jones PS, et al. Neuroinflammation predicts disease progression in progressive supranuclear palsy. J Neurol Neurosurg Psychiatry 2021;92(7):769–775.
24. Kübler D, Wächter T, Cabanel N, et al. Widespread microglial activation in multiple system atrophy. Mov Disord 2019;34(4):564–568.
25. Hoffmann A, Ettle B, Battis K, et al. Oligodendroglial α-synucleinopathy-driven neuroinflammation in multiple system atrophy. Brain Pathol 2019;29(3):380–396.
26. Ono M, Takahashi M, Shimozawa A, et al. In vivo visualization of propagating α-synuclein pathologies in mouse and marmoset models by a bimodal imaging probe, C05-05. bioRxiv 2021;
27. Shahnawaz M, Mukherjee A, Pritzkow S, et al. Discriminating alpha-synuclein strains in Parkinson's disease and multiple system atrophy. Nature 2020;578(7794):273–277.
28. Jansen WJ, Janssen O, Tijms BM, et al. Prevalence estimates of amyloid abnormality across the Alzheimer disease clinical Spectrum. JAMA Neurol 2022;79(3):228–243.
29. Homma T, Mochizuki Y, Tobisawa S, Komori T, Isozaki E. Cerebral white matter tau-positive granular glial pathology as a characteristic pathological feature in long survivors of multiple system atrophy. J Neurol Sci 2020;416:117010

Supporting Data

Additional Supporting Information may be found in the online version of this article at the publisher's web-site.

SGML and CITI Use Only
DO NOT PRINT

Author Roles

(1) Research Project: A. Conception, B. Organization, C. Execution; (2) Statistical Analysis: A. Design, B. Execution, C. Review and Critique; (3) Manuscript: A. Writing of the First Draft, B. Review and Critique.

F.-T.L.: 1A, 1B, 1C, 2A, 2B, 2C, 3A, 3B
X.-Y.L.: 1A, 1B, 1C, 2A, 2B, 2C, 3A, 3B
J.-Y.L.: 1A, 1B, 1C, 2A, 2B, 2C, 3A, 3B
P.W.: 1A, 1B, 1C, 2A, 2C, 3B
L.L.: 1A, 1B, 1C, 2A, 2C, 3B
X.-N.L.: 1A, 1B, 1C, 2A, 2C, 3B
Z.-Z.J.: 1A, 1B, 1C, 2A, 2C, 3B
F.-Y.J.: 1A, 1B, 1C, 2A, 2C, 3B
M.-J.C.: 1A, 1B, 1C, 2A, 2C, 3B
J.-J.G.: 1A, 1B, 1C, 2A, 2C, 3B
Y.-M.S.: 1A, 1B, 1C, 2C, 3B
J.-J.W.: 1A, 1B, 1C, 2C, 3B
T.-C.Y.: 1A, 1B, 1C, 2C, 3B
J.-F.L.: 1A, 1B, 1C, 2C, 3B
C.Z.: 1A, 1B, 1C, 2C, 3B
J.W.: 1A, 1B, 1C, 2C, 3B

Full financial disclosures for the previous 12 months

None.